Enhanced coercivity in B-rich nanocomposite α-Fe/$(NdPr)_2Fe_{14}B$/Fe_3B hard magnetic alloys

I. Betancourt[a)]
Instituto de Investigaciones en Materiales, Universidad Nacional Autónoma de México, P.O. Box 70-360, México DF 04510

H. A. Davies
Department of Engineering Materials, University of Sheffield, Portobello Street, Sheffield S1 3JD, United Kingdom

(Received 19 April 2005; accepted 24 August 2005; published online 14 October 2005)

The structures and magnetic properties of melt-spun B-rich (10 at. %) and Nb-containing nanocomposite alloys, with compositions based on the formula $(Nd_{0.75}Pr_{0.25})_yFe_{90-y-x}Nb_xB_{10}$ ($y=8$, 10; $x=0$, 2, 4) have been studied. Considerable enhancement of the intrinsic coercivity, (of 657 kA/m) together with excellent energy density (of 113 kJ/m^3), were observed for $y=8$, $x=4$; while for $y=10$ and $x=2$, values of 912 kA/m and 140 kJ/m^3 were attained. Results are interpreted in terms of a grain size refining effect of the Nb addition and to the more complete exchange coupling of the soft grains to the hard phase grains afforded by reduced grain sizes. © *2005 American Institute of Physics*. [DOI: 10.1063/1.2106004]

Nanocomposite exchange-enhanced hard magnetic alloys have been intensively studied since their first experimental and theoretical description.[1–3] These alloys are comprised of a fine mixture of hard magnetic crystallites [$RE_2Fe_{14}B$,[2,3] $RE_2Fe_{17}N_x$,[4] or $RE_2Fe_{17}C_x$, (Ref. 5) rare earth (RE)=Nd or Pr] interspersed with soft magnetic grains [α-Fe (Refs. 3–5) or Fe_3B.[2]) The corresponding soft/hard mean grain sizes should ideally be of 10 nm for the soft phase and 20 nm for the hard phase, according to numerical simulations,[6] in order to avoid independent magnetization reversal at the soft grains and thus, promote optimum ferromagnetic exchange coupling between hard and soft magnetic phases. Such exchange interaction leads to enhanced values of remanence, J_r, to well above the Stoner–Wohlfarth value of $0.5J_s$, but with reduced intrinsic coercivity ${}_iH_c$ (within the range of 250–500 kA/m, depending on composition). Furthermore, their reduced RE content decreases the raw material cost, which represents a useful advantage for commercial purposes. For the melt-spun alloys with intermediate RE concentrations (8–11 at. %) and a stoichiometric B content of ~6 at. %, produced by direct quenching from the liquid state, the high cooling rate during the rapid solidification facilitates very large undercoolings and very high nucleation frequencies for both $RE_2Fe_{14}B$ and α-Fe crystallites. This yields very fine-grained structures with optimum magnetic properties. However, a major practical impediment for the full exploitation of this class of nanocomposite alloy is the narrow process window and the tendency to produce a range of ribbon thicknesses in a batch, and thus with variable microstructure and properties.[7] An alternative process route is to "overquench" the alloy to the fully amorphous state followed by a devitrification anneal. This has been shown to give broadly comparable microstructures and magnetic properties to those obtained by direct quenching for stoichiometric $RE_2Fe_{14}B$ alloys.[8,9] However, for overquenched initially amorphous REFeB alloys with Fe-rich compositions (RE content <11.7 at. %), the microstructural evolution upon annealing begins with the precipitation and growth of α-Fe grains[10–12] followed by the formation and growth of the $RE_2Fe_{14}B$ crystallites. This process tends to result in undesirably coarse α-Fe crystallites, which leads to incomplete exchange coupling to the hard phase grains and, thus, to inferior magnetic properties for the composite structure.[10,13] The addition of small concentrations of refractory elements (Zr or Nb) has been reported to be useful for controlling the growth of the soft phase.[14,15] Moreover, an excess of B content has also been reported as having an enhancing effect on intrinsic coercivity for nancomposite α-Fe/REFeB alloys with RE concentrations ⩾10 at. %.[16,17] In the present letter, we report the effects of both an excess concentration of B (10 at. %) and of Nb additions (up to 4 at. %) on the microstructure and magnetic properties of nanocomposite α-Fe/REFeB alloys with RE=8 and 10 at. %.

Ingots of the alloys, with compositions of $RE_yFe_{90-y-x}Nb_xB_{10}$ ($RE=Nd_{0.75}Pr_{0.25}$, $y=8$, 10; $x=0$, 2, 4),

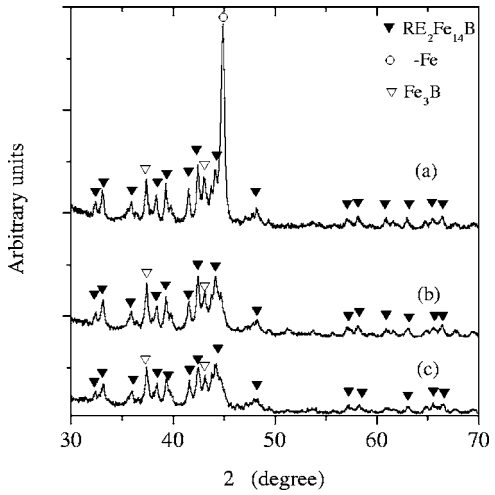

FIG. 1. XRD traces for ribbon samples of the alloy series $(Nd_{0.75}Pr_{0.25})_{10}Fe_{80-x}Nb_xB_{10}$, spun at 30 m/s and annealed at 700 °C for 10 min: (a) $x=0$, (b) $x=2$, and (c) $x=4$.

[a)]Author to whom correspondence should be addressed; electronic mail: israelb@correo.unam.mx

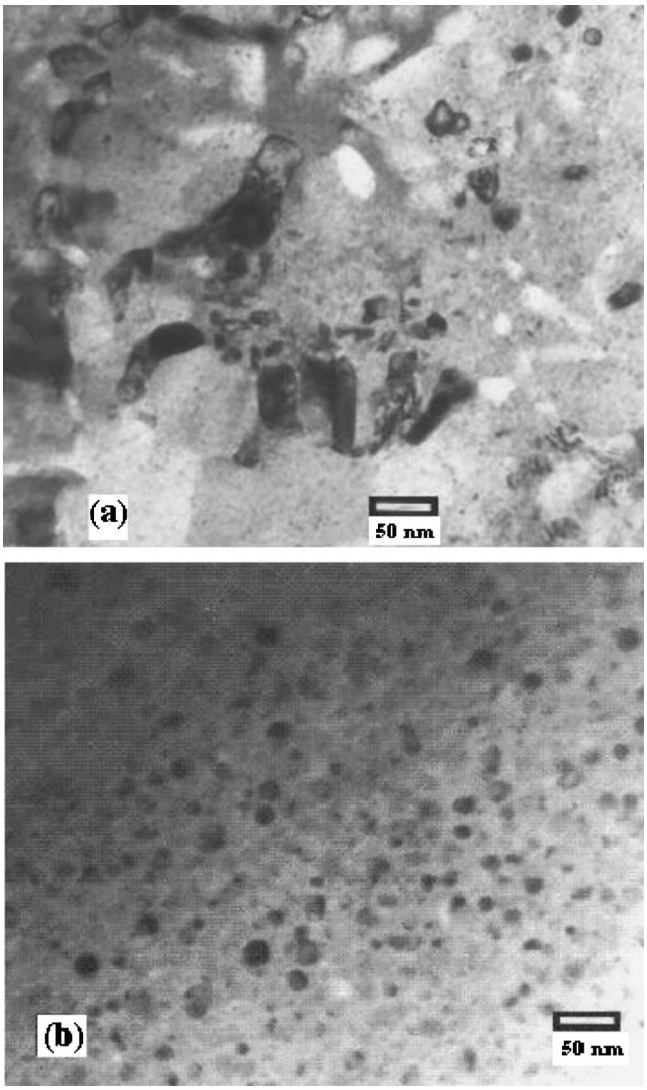

FIG. 2. TEM micrograph for selected OA nanocomposite: (a) $RE_8Fe_{82}B_{10}$ and (b) $RE_8Fe_{78}Nb_4B_{10}$ ribbon samples.

were prepared using commercial grade materials by arc melting the constituents in a high-purity Ar atmosphere. Overquenched and annealed (OA) samples were obtained by a devitrification anneal (10 min at 700 °C with material sealed in a silica tube under argon) of initially fully amorphous alloy ribbon, produced by melt spinning at 30 m/s. The magnetic properties of J_r and ${}_iH_c$, and the maximum energy product $(BH)_{\max}$, were determined using an Oxford vibrating sample magnometer with a maximum field of 5 T. The microstructure of selected ribbon samples was monitored by x-ray diffraction (XRD) analysis with Cu $K\alpha$ radiation and transmission electron microscopy (TEM).

Diffractograms for the $RE_{10}Fe_{80-x}Nb_xB_{10}$ ($x=0$, 2, 4) series are shown in Fig. 1. For the Nb-free alloy, the presence of the body-centered-cubic α-Fe phase is manifested as a strong diffraction peak at $2\theta=44.6°$ [corresponding to the (110) reflection] together with peaks for the 2/14/1 hard phase. In addition, a peak at $2\theta=42.99°$ can be indexed as (321) for the Fe_3B phase, which has the highest intensity for this phase. As the Nb content increases, the intensity of the α-Fe peak exhibits a progressive decrease, reflecting the effect of Nb as a grain size controller. Similar results were observed for the alloy series with RE=8 at. % (not included). Transmission electron micrographs for two selected

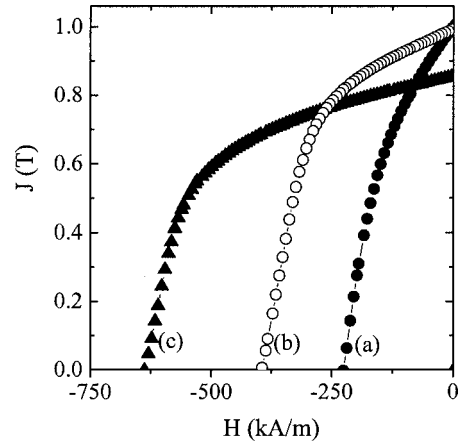

FIG. 3. Demagnetizing curves for OA ribbon samples of alloys in the system $RE_8Fe_{82-x}Nb_xB_{10}$: (a) $x=0$, (b) $x=2$, and (c) $x=4$.

nanocomposite alloys, $RE_8Fe_{82}B_{10}$ and $RE_8Fe_{78}Nb_4B_{10}$, are displayed in Fig. 2. For the Nb-free sample, Fig. 2(a) shows a nanostructure comprised of smaller grains (<15 nm, presumably hard 2/14/1 phase) and much larger crystallites (>50 nm, evidently α-Fe, due to their dislocated internal structure), while for the alloy with 4 at. % of Nb [Fig. 2(b)], a homogeneous grain size distribution, with mean grain diameters for both soft and hard phases of <25 nm, reflects the grain size controlling effect of the Nb addition. The second quadrants of the *J-H* loops for all alloys investigated are shown in Figs. 3 and 4. For the RE=8 at. % series (Fig. 3), ${}_iH_c$ increases progressively as the Nb concentration increases, from 228 kA/m ($x=0$) to 657 kA/m ($x=4$), though with a marked reduction in J_r between 2 and 4 at. % Nb. $(BH)_{\max}$ is increased significantly upon adding Nb, from 60 kJ/m^3 up to 117 kJ/m^3 for the 2 at. % Nb alloy, with a slight drop upon increasing to 4 at. %. The observed values of J_r and ${}_iH_c$, and the derived values of $(BH)_{\max}$, for each composition are given in Table I. For the RE=10 at. % series (Fig. 4), consistently larger ${}_iH_c$ values were observed, ranging from 619 kA/m for the Nb-free alloy to 1060 kA/m for the 4 at. % Nb composition, reflecting the smaller volume fraction of soft magnetic phases present, and with $(BH)_{\max}$ being as high as 140 kJ/m^3 for the 2 at. % Nb alloy. Table I summarizes these experimental data.

It is observed that the addition of up to 4 at. % Nb substantially enhances ${}_iH_c$, and improves the squareness of the

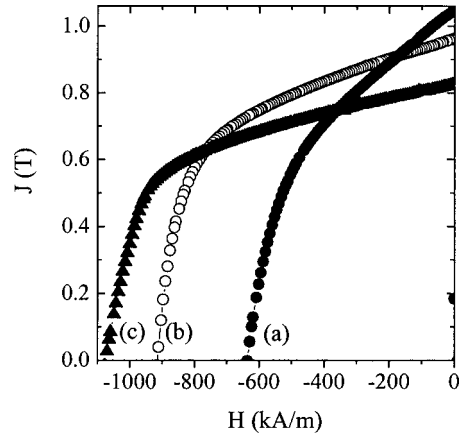

FIG. 4. Demagnetizing curves for OA ribbon samples of alloys in the system $RE_{10}Fe_{80-x}Nb_xB_{10}$: (a) $x=0$, (b) $x=2$, and (c) $x=4$.

TABLE I. Magnetic properties of OA ribbon samples of alloys in the system $(Nd_{0.75}Pr_{0.25})_yFe_{90-y-x}Nb_xB_{10}$ (mean values for ten samples in each case).

RE content y, Nb content x	${}_iH_c$ (kA/m)	J_r (T)	J_s (T)	$(BH)_{max}$ (kJ/m^3)
$y=8$, $x=0$	228±10	1.04±0.06	1.75±0.04	60±7
$y=8$, $x=2$	420±20	0.98±0.04	1.56±0.06	117±5
$y=8$, $x=4$	657±10	0.87±0.01	1.31±0.01	113±2
$y=10$, $x=0$	619±24	1.05±0.02	1.60±0.02	128±9
$y=10$, $x=2$	912±5	0.96±0.01	1.47±0.02	140±6
$y=10$, $x=4$	1060±18	0.81±0.01	1.24±0.01	109±3

loops due to a narrow grain size distribution, which explains the good $(BH)_{max}$ values, in spite of the modest J_r values attained. These modest J_r values result from a moderated diluting effect of the 2/14/1 phase induced by the rising Nb concentration. The ${}_iH_c$ increment, observed with increasing Nb content, can be ascribed to the considerable grain size refinement—notably of the soft phase—promoted by the Nb. This effect has been described by micromagnetic simulations for nanocomposite α-Fe/$Nd_2Fe_{14}B$ alloys.[18,19] According to these simulations, ${}_iH_c$ is predicted to increase with decreasing soft/hard mean grain sizes due to the enhanced intergrain exchange interactions between the two phases. This is expected to suppress the nucleation of reverse domains within the soft grains, thus retarding the magnetization reversal of the neighboring hard grains to higher applied fields and giving rise to improved ${}_iH_c$ values. The tendency for ${}_iH_c$ to increase with decreasing grain size was previously observed experimentally for Nb-free intermediate ${}_iH_c$ (<400 kA/m) nanocomposite α-Fe/$Nd_2Fe_{14}B$ alloys with a soft phase volume fraction of 30%.[20]

In summary, a marked enhancement of ${}_iH_c$ (up to 1060 kA/m) was observed upon the addition of Nb to B-rich melt-spun nanocomposite $RE_2Fe_{14}B/\alpha$-Fe/Fe_3B alloys. TEM observations revealed a considerable grain size refining effect promoted by the Nb additions, which is considered to be responsible for the increased ${}_iH_c$. This ${}_iH_c$ enhancement, in addition to the improved squareness of the demagnetizing curves, resulted in good maximum energy densities (up to 140 kJ/m^3 for the $RE_{10}Fe_{78}Nb_2B_{10}$ composition), thus rendering this alloy series a promising candidate for bonded magnet applications.

The authors are grateful to The Royal Society for the financial support of one author's (I. B.) visit to the University of Sheffield. That same author acknowledges research funding through project IN119603-UNAM and the helpful technical assistance from Mr. C. Flores.

[1] R. Coehoorn, D. B. de Mooij, J. P. W. B. Duchateau, and K. H. J. Buschow, J. Phys. **C8**, 669 (1988).
[2] E. Kneller and R. Hawig, IEEE Trans. Magn. **27**, 3588 (1991).
[3] A. Manaf, R. A. Buckley, and H. A. Davies, J. Magn. Magn. Mater. **128**, 302 (1993).
[4] J. Ding, P. G. McCormick, and R. Street, J. Magn. Magn. Mater. **124**, 1 (1993).
[5] Z. M. Chen, C. Y. Ni, and G. C. Hadjipanayis, J. Magn. Magn. Mater. **186**, 41 (1998).
[6] R. Fischer, T. Schrefl, H. Kronmuller, and J. Fidler, J. Magn. Magn. Mater. **153**, 35 (1996).
[7] H. A. Davies, *Proceedings of the Eighth Symposium on Magnetic Anisotropy and Coercivity in RE-TM Alloys*, edited by C. A. F. Manwaring, D. G. R. Jones, A. J. Williams, and I. R. Harris, (University of Birmingham, UK, 1994) p. 465.
[8] H. A. Davies, C. L. Harland, J. I. Betancourt, and G. Mendoza, *Proceedings of the MRS Symposium on Advanced Hard and Soft Magnetic Materials*, edited by M. Coey, L. H. Lewis, B. M. Ma, T. Schrefl, L. Schultz, J. Fidler, V. G. Harris, R. Hasegawa, A. Inoue, and M. McHenry, (Materials Research Society, Warrendale, PA, 1999) p. 27.
[9] C. L. Harland and H. A. Davies, J. Appl. Phys. **87**, 6116 (2000).
[10] A. Kojima, F. Ogiwara, A. Makino, A. Inoue, and T. Masumoto, Mater. Sci. Eng., A **226**, 520 (1997).
[11] Z. Wang, S. Zhou, M. Zhang, Y. Quiao, and R. Wang, J. Appl. Phys. **86**, 7010 (1999).
[12] Z. Wang, S. Zhou, M. Zhang, Y. Quiao, X. Gao, Q. Zhao, R. Wang, and W. Gong, J. Appl. Phys. **85**, 4880 (1999).
[13] A. M. Gabay, A. G. Popov, V. S. Gaviko, Y. V. Belozerov, and A. S. Yermolenko, J. Alloys Compd. **245**, 119 (1996).
[14] I. Betancourt and H. A. Davies, J. Magn. Magn. Mater. **261**, 328 (2003).
[15] Z. Chen, Y. Zhang, Y. Ding, and G. C. Hadjipanayis, J. Appl. Phys. **85**, 5908 (1999).
[16] W. C. Chang, D. Y. Chiou, S. H. Wu, B. M. Ma, and C. O. Bounds, Appl. Phys. Lett. **72**, 121 (1998).
[17] W. C. Chang, S. H. Wang, S. J. Chang, M. Y. Tsai, and B. M. Ma, IEEE Trans. Magn. **35**, 3265 (1999).
[18] T. Schrefl, R. Fischer, J. Fidler, and H. Kronmuller, J. Appl. Phys. **76**, 7053 (1994).
[19] R. Fischer, T. Schrefl, H. Kronmuller, and J. Fidler, J. Magn. Magn. Mater. **153**, 35 (1996).
[20] J. I. Betancourt and H. A. Davies, J. Magn. Magn. Mater. **246**, 6 (2002).